Article

Magnetic Moment of Cu-Modified Ni₂MnGa Magnetic Shape Memory Alloys

Takeshi Kanomata [1,2], Keita Endo [3], Naoto Kudo[3], Rie Y. Umetsu [4,5,*], Hironori Nishihara [6], Mitsuo Kataoka [7], Makoto Nagasako [8], Ryosuke Kainuma [8] and Kurt R.A. Ziebeck [9]

[1] Research Institute for Engineering and Technology, Tohoku Gakuin University, Tagajo 985-8537, Japan; E-Mail: kanomata@tjcc.tohoku-gakuin.ac.jp

[2] Department of Materials Science, Graduate School of Engineering, Tohoku University, Sendai 980-8579, Japan

[3] Faculty of Engineering, Tohoku Gakuin University, Tagajo 985-8537, Japan; E-Mails: e.keita.g@gmail.com (K.E.); nimncuga@live.jp (N.K.)

[4] Institute for Materials Research, Tohoku University, Sendai 980-8577, Japan

[5] Japan Science and Technology Agency-Precursory Research for Embryonic Science and Technology (JST-PREST), Tokyo 102-0076, Japan

[6] Faculty of Science and Technology, Ryukoku University, Otsu 520-2194, Japan; E-Mail: nishihara@rins.ryukoku.ac.jp

[7] Department of Basic Sciences, Faculty of Science and Engineering, Ishinomaki Senshu University, Ishinomaki 986-8580, Japan; E-Mail: kataokam@kxe.biglobe.ne.jp

[8] Department of Materials Science, Graduate School of Engineering, Tohoku University, Sendai 980-8579, Japan; E-Mails: nagasako@material.tohoku.ac.jp (M.N.); kainuma@material.tohoku.ac.jp (R.K.)

[9] Department of Physics, Cavendish Laboratory, University of Cambridge, Cambridge CB3 0HE, UK; E-Mail: kraz2@cam.ac.uk

* Author to whom correspondence should be addressed; E-Mail: rieume@imr.tohoku.ac.jp; Tel.: +81-22-215-2492; Fax: +81-22-215-2381.

Abstract: The magnetization measurements at 5 K were carried out for $Ni_2Mn_{1-x}Cu_xGa$ ($0 \leq x \leq 0.40$) and $Ni_2MnGa_{1-y}Cu_y$ ($0 \leq y \leq 0.25$) alloys. All of the magnetization curves are characteristic of ferromagnetism or ferrimagnetism. By using Arrott plot analysis the spontaneous magnetization of all samples was determined from the magnetization curves. The magnetic moment per formula unit, μ_s, at 5 K was estimated from the spontaneous

magnetization. For $Ni_2Mn_{1-x}Cu_xGa$ ($0 \leq x \leq 0.40$) alloys μ_s at 5 K decreases linearly with increasing x. On the other hand, the μ_s at 5 K for $Ni_2MnGa_{1-y}Cu_y$ ($0 \leq y \leq 0.25$) alloys decreases more steeply with increasing x compared to the μ_s for $Ni_2Mn_{1-x}Cu_xGa$ ($0 \leq x \leq 0.40$) alloys. On the basis of the experimental results, the site-occupation configurations of $Ni_2Mn_{1-x}Cu_xGa$ ($0 \leq x \leq 0.40$) and $Ni_2MnGa_{1-y}Cu_y$ ($0 \leq y \leq 0.25$) alloys are proposed.

Keywords: magnetic shape memory alloy; Heusler alloy; Ni_2MnGa; magnetic moment

---

1. Introduction

In recent years, Heusler alloys have become a subject of intensive experimental and theoretical investigations. Ferromagnetic shape memory alloys (FSMAs) with the Heusler-type structure ($L2_1$-type structure), which exhibit both the ferromagnetic and structural transitions, have attracted much attention due to their potential application as smart materials [1,2]. A large magnetic field-induced strain by the rearrangement of twin variants in the martensite phase was observed in the Ni-Mn-Ga FSMAs [3,4]. Moreover, a large magnetocaloric effect (MCE) accompanied by a magnetostructural transition, where both the ferromagnetic and structural transitions occur together, has been expected to be useful for devices [5,6]. Among FSMAs, the stoichiometric Heusler alloy Ni_2MnGa has been the most studied. Ni_2MnGa orders ferromagnetically with a Curie temperature of $T_C \approx 365$ K. On cooling below the martensitic transition temperature $T_M \approx 200$ K, a superstructure forms, and the ferromagnetic state remains below T_M [7,8]. The spontaneous magnetization M_s just below T_M is larger than the M_s just above T_M for Ni_2MnGa.

Recently, Kataoka *et al*. [9] and Endo *et al*. [10] carried out magnetization, permeability and differential scanning calorimetric (DSC) measurements on the FMSAs $Ni_2Mn_{1-x}Cu_xGa$ ($0 \leq x \leq 0.40$) and $Ni_2MnGa_{1-y}Cu_y$ ($0 \leq y \leq 0.25$) alloys, respectively. It was found that for $Ni_2Mn_{1-x}Cu_xGa$ ($0 \leq x \leq 0.40$) alloys the magnetostructural transitions between the paramagnetic austenite phase (Para-A) and the ferromagnetic martensite phase (Ferro-M) occur in the concentration range of $0.23 \leq x \leq 0.30$ [9]. Similarly, the magnetostructural transitions between the Para-A and Ferro-M were observed in the concentration range of $0.12 \leq y \leq 0.14$ for $Ni_2MnGa_{1-y}Cu_y$ ($0 \leq y \leq 0.25$) alloys [10]. Furthermore, the characteristics of the phase diagrams of $Ni_2Mn_{1-x}Cu_xGa$ ($0 \leq x \leq 0.40$) and $Ni_2MnGa_{1-y}Cu_y$ ($0 \leq y \leq 0.25$) alloys were found to be very similar to those of $Ni_{2+x}Mn_{1-x}Ga$ ($0 \leq x \leq 0.36$) alloys [11]. Kataoka *et al*. explained the phase diagram of $Ni_2Mn_{1-x}Cu_xGa$ ($0 \leq x \leq 0.40$) alloys using the Landau-type phenomenological free energy as a function of the martensitic distortion and the magnetization [9]. Their analysis showed that the biquadratic coupling term, together with a higher order term, of the martensitic distortion and the magnetization plays an important role in the interplay between the martensite phase and the ferromagnetic phase. As the result, Kataoka *et al*. could obtain the satisfactory agreement between the calculated and observed phase diagrams for $Ni_2Mn_{1-x}Cu_xGa$ ($0 \leq x \leq 0.40$) alloys. Also the phase diagram of $Ni_{2-z}Cu_zMnGa$ ($0 \leq z \leq 0.8$) alloys was determined from the results of the temperature dependence of the initial

permeability [12]. The T_C of $Ni_{2-z}Cu_zMnGa$ ($0 \leq z \leq 0.8$) alloys increased with the Cu concentration z. While, the T_M decreased abruptly with z.

In this paper, the concentration dependence of the magnetic moment for $Ni_2Mn_{1-x}Cu_xGa$ ($0 \leq x \leq 0.40$) and $Ni_2MnGa_{1-y}Cu_y$ ($0 \leq y \leq 0.25$) alloys is examined to gain deeper insight for the magnetic properties of these FSMAs. On the basis of the experimental results, the site occupancy and the magnetic structure of $Ni_2Mn_{1-x}Cu_xGa$ ($0 \leq x \leq 0.40$) and $Ni_2MnGa_{1-y}Cu_y$ ($0 \leq y \leq 0.25$) alloys are presented. Furthermore, the site occupancy of $Ni_{2-z}Cu_zMnGa$ ($0 \leq z \leq 0.4$) alloys is also presented.

2. Experimental Section

The $Ni_2Mn_{1-x}Cu_xGa$ ($0 \leq x \leq 0.40$) and $Ni_2MnGa_{1-y}Cu_y$ ($0 \leq y \leq 0.25$) alloys were prepared by repeated arc melting of the constituent elements, namely 99.99% pure Ni, 99.99% pure Mn, 99.99% pure Cu and 99.9999% pure Ga in argon atmosphere. The heat treatments of all reaction products after the arc melting were reported in the references [9,10]. Weight loss between before and after the arc melting is within 0.5%, thus the composition of the specimens is seen to be the same with the nominal ones. By using X-ray powder diffraction measurements all samples were confirmed to be of single phase at room temperature. Magnetization measurements on prepared samples were carried out in magnetic fields up to 50 kOe using a superconducting quantum interference device (SQUID) magnetometer.

3. Results and Discussion

Figures 1 and 2 show the phase diagrams of $Ni_2Mn_{1-x}Cu_xGa$ ($0 \leq x \leq 0.40$) and $Ni_2MnGa_{1-y}Cu_y$ ($0 \leq y \leq 0.25$) alloys reported by Kataoka *et al.* [9] and Endo *et al.* [10], respectively. The phase diagrams shown in Figures 1 and 2 have characteristics very similar to that [11] of $Ni_{2+x}Mn_{1-x}Ga$ ($0 \leq x \leq 0.36$) alloys. As shown in Figure 1, the samples with $x \leq 0.20$ of $Ni_2Mn_{1-x}Cu_xGa$ ($0 \leq x \leq 0.40$) alloys crystallize in the $L2_1$-type structure at room temperature. However, the details of the crystal structure in the martensite phase for the samples with $x \leq 0.20$ are not clear. It was confirmed by the low temperature X-ray powder diffraction measurements that the sample with $x = 0.23$ for $Ni_2Mn_{1-x}Cu_xGa$ alloy crystallizes in a 14-layered monoclinic (14*M*) structure (space group: $C2/m$) well below the martensitic transition temperature [9]. The X-ray powder diffraction pattern of the sample with $x = 0.23$ at room temperature shows that the cubic phase with the $L2_1$-type structure and the monoclinic phase with the 14*M* structure coexist. Similarly, the X-ray powder diffraction patterns at room temperature of the samples with $x = 0.25$ and 0.27 indicated that the $L2_1$ phase and the 14*M* phase coexist although the fraction of the 14*M* phase increases with increasing the concentration x. The sample with $x = 0.35$ crystallizes in a tetragonal $D0_{22}$-like crystal structure with no lattice modulation at room temperature. The crystal structures of the 14*M* and the $D0_{22}$-like also appear in the martensite phase of $Ni_2MnGa_{1-y}Cu_y$ ($0 \leq y \leq 0.25$) alloys depending on the Cu concentration, being similar to that of $Ni_2Mn_{1-x}Cu_xGa$ ($0 \leq x \leq 0.40$) alloys [10]. The magnetization curves at 5 K for $Ni_2Mn_{1-x}Cu_xGa$ ($0 \leq x \leq 0.40$) alloys with various concentrations x are shown in Figure 3. All of the magnetization curves are characteristic of ferromagnetism or ferrimagnetism. The magnetization *M* at 5 K for all samples is saturated in a field of about 20 kOe. The magnetization curves at 5 K for $Ni_2MnGa_{1-y}Cu_y$ ($0 \leq y \leq 0.25$) alloys with various concentrations y are shown in Figure 4. The

spontaneous magnetization at 5 K for $Ni_2Mn_{1-x}Cu_xGa$ ($0 \leq x \leq 0.40$) and $Ni_2MnGa_{1-y}Cu_y$ ($0 \leq y \leq 0.25$) alloys was determined by the linear extrapolation to $H/M = 0$ of the M^2 versus H/M curves (Arrott plot). The magnetic moments per formula unit, μ_s, at 5 K for $Ni_2Mn_{1-x}Cu_xGa$ ($0 \leq x \leq 0.40$) and $Ni_2MnGa_{1-y}Cu_y$ ($0 \leq y \leq 0.25$) alloys were estimated from the values of the spontaneous magnetization and are plotted against concentrations x and y as shown in Figure 5. The concentration dependence of μ_s at 5 K for $Ni_{2-z}Cu_zMnGa$ ($0 \leq z \leq 0.40$) alloys is also shown in Figure 5 [12], where the values of μ_s for $Ni_{2-z}Cu_zMnGa$ ($0 \leq z \leq 0.40$) alloys were determined at 4.2 K. The μ_s at 5 K of the stoichiometric Ni_2MnGa is estimated to be about 4 μ_B/f.u. by extrapolations of the μ_s *versus x* curve for $Ni_2Mn_{1-x}Cu_xGa$ ($0 \leq x \leq 0.40$) alloys to $x = 0$ and of the μ_s *versus y* curve for $Ni_2MnGa_{1-y}Cu_y$ ($0 \leq y \leq 0.25$) alloys to $y = 0$. Recently, Ahuja *et al.* carried out a magnetic Compton scattering study of the near-stoichiometric Heusler alloy $Ni_{2.03}Mn_{0.97}Ga$ [13]. For $Ni_{2.03}Mn_{0.97}Ga$, they found the value of μ_s to be 4.01 μ_B/f.u. at 110 K in a field of 2 T. The value of μ_s at 5 K for Ni_2MnGa in the present study is in good agreement with the value reported by Ahuja *et al.* [13].

Figure 1. Phase diagram of $Ni_2Mn_{1-x}Cu_xGa$ ($0 \leq x \leq 0.4$) alloys [9]. Para and Ferro mean the paramagnetic and ferromagnetic state, respectively. A and M represent the austenite and martensite phases, respectively. T_p is the premartensitic transition temperature. T_C and T_M are the Curie temperature and the martensitic transition temperature, respectively.
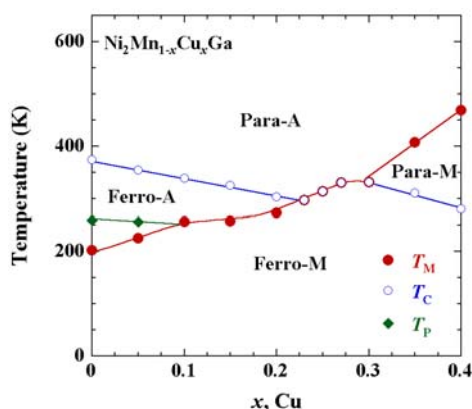

Figure 2. Phase diagram of $Ni_2MnGa_{1-y}Cu_y$ ($0 \leq y \leq 0.25$) alloys [10]. Para and Ferro mean the paramagnetic state and ferromagnetic one, respectively. A and M represent the austenitic and martensitic phases, respectively. T_C, T_M and T_p are the Curie temperature, the martensitic transition temperature, and premartensitic transition temperature, respectively.
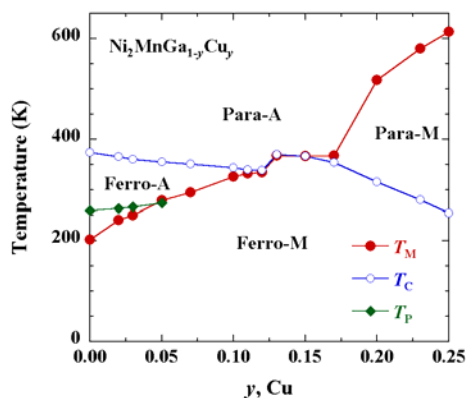
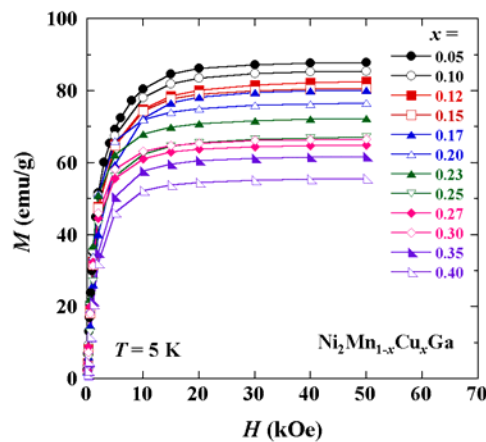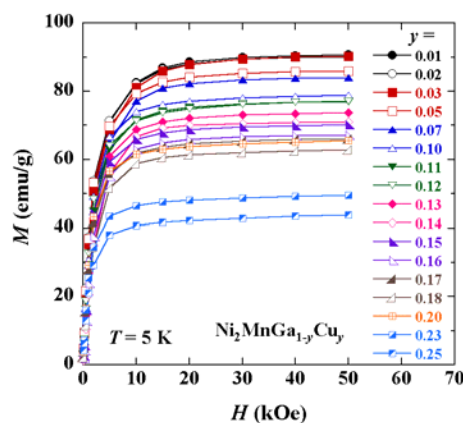**Figure 3.** Magnetization curves at 5 K for $Ni_2Mn_{1-x}Cu_xGa$ ($0 \leq x \leq 0.40$) alloys with various concentration x.

Figure 4. Magnetization curves at 5 K for $Ni_2MnGa_{1-y}Cu_y$ ($0 \leq y \leq 0.25$) alloys with various concentration y.

Recently, Li *et al.* investigated theoretically the site preference and elastic properties of Fe-, Co- and Cu-doped Ni_2MnGa alloys by using the first-principles exact muffin-tin orbital method in combination with the coherent-potential approximation [14]. According to the results of the calculation by Li *et al.* [14], Cu atoms for $Ni_2Mn_{0.95}Cu_{0.05}Ga$ occupy the vacant Mn sublattice and the magnetic moments of the Ni, Mn, Cu and Ga atoms, μ_{Ni}, μ_{Mn}, μ_{Cu} and μ_{Ga}, in $Ni_2Mn_{0.95}Cu_{0.05}Ga$ are 0.32 μ_B, 3.37 μ_B, -0.03 μ_B and -0.05 μ_B, respectively. The values of μ_{Ni}, μ_{Mn} and μ_{Ga} calculated by Li *et al.* [14] are in good agreement with those reported earlier for the stoichiometric Heusler alloy Ni_2MnGa [15–22]. In order to explain the observed concentration dependence of the magnetic moment for $Ni_2Mn_{1-x}Cu_xGa$ ($0 \leq x \leq 0.40$) alloys we present a simple model in which the following assumptions are made. Cu atoms for $Ni_2Mn_{1-x}Cu_xGa$ ($0 \leq x \leq 0.40$) alloys always occupy the vacant Mn sublattice. The magnetic moments of the Ni, Mn, Cu and Ga atoms in $Ni_2Mn_{1-x}Cu_xGa$ ($0 \leq x \leq 0.40$) alloys are collinear and have Li *et al.*'s values independent of x. The magnetic moments of the Mn atoms are ferromagnetically coupled to the magnetic moments of the Ni atoms. Then, the total magnetic moment per formula unit, μ_s (cal), of $Ni_2Mn_{1-x}Cu_xGa$ ($0 \leq x \leq 0.40$) alloys is given by $\mu_s(cal) = 2\mu_{Ni} + (1-x)\mu_{Mn} + x\mu_{Cu} + \mu_{Ga}$. The solid line in Figure 5 is the one calculated by using this equation. As seen in Figure 5, the experimental values are in good agreement with those calculated.

Figure 5. Concentration dependence of the magnetic moment per formula unit, μ_s, for $Ni_2Mn_{1-x}Cu_xGa$ ($0 \leq x \leq 0.40$), $Ni_2MnGa_{1-y}Cu_y$ ($0 \leq y \leq 0.25$) and $Ni_{2-z}Cu_zMnGa$ ($0 \leq z \leq 0.40$). All values of μ_s were determined at 5 K except for the values of μ_s of $Ni_{2-z}Cu_zMnGa$ ($0 \leq z \leq 0.40$) alloys. They were estimated at 4.2 K [12].
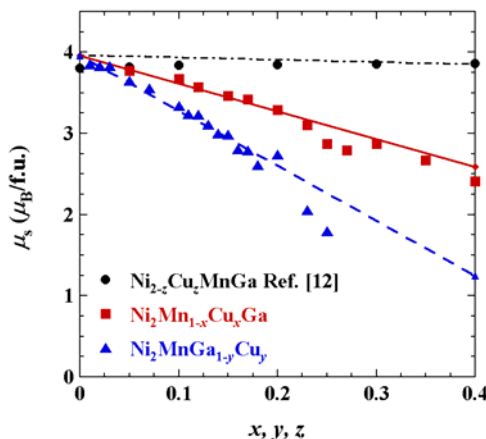
Next, we consider the concentration dependence of μ_s for $Ni_2MnGa_{1-y}Cu_y$ ($0 \leq y \leq 0.25$) alloys. According to the results of the calculation for the site occupation of $Ni_2MnGa_{0.95}Cu_{0.05}$ by Li *et al.* [14], Cu atoms always occupy the sublattice of the deficient component; the configuration $Ni_2Mn(Ga_{0.95}Cu_{0.05})$ is the most stable in where the components A and B in (A,B) occupy the same sublattice. In this case, the μ_s at 5 K for $Ni_2MnGa_{1-y}Cu_y$ ($0 \leq y \leq 0.25$) alloys is almost independent of *y* under the assumption that $Ni_2MnGa_{1-y}Cu_y$ ($0 \leq y \leq 0.25$) alloys are collinear ferromagnets and the values of μ_{Ni} and μ_{Mn} are independent of *x*. However, as shown in Figure 5, the experimental μ_s at 5 K for $Ni_2MnGa_{1-y}Cu_y$ ($0 \leq y \leq 0.25$) alloys decreases steeply with increasing *y*. We, therefore, suggest a different site-occupation configuration *i.e.*, $Ni_2(Mn_{1-y}Cu_y)(Ga_{1-y}Mn_y)$ with the Cu atoms occupying the Mn sublattice, for $Ni_2MnGa_{1-y}Cu_y$ ($0 \leq y \leq 0.25$) alloys, where some of the Mn atoms move on to the Ga sublattice. Here, we assume that the magnetic moment of the Mn atoms substituted on to the Ga sites in $Ni_2(Mn_{1-y}Cu_y)(Ga_{1-y}Mn_y)$ alloys is antiferomagnetically coupled to the magnetic moment of the Mn atoms on the Mn sublattice. The values of the magnetic moments of the Mn atoms on the Mn and Ga sublattices, respectively, are assumed to be 3.37 μ_B and -3.43 μ_B, which remain constant with increasing *y* from *y* = 0. The other magnetic moments μ_{Ni}, μ_{Cu} and μ_{Ga} in the $Ni_2(Mn_{1-y}Cu_y)(Ga_{1-y}Mn_y)$ alloys are the constant values 0.32 μ_B, -0.03 μ_B and -0.05 μ_B, respectively, as in $Ni_2Mn_{1-x}Cu_xGa$ ($0 \leq x \leq 0.40$) alloys. A value of -3.43 μ_B was calculated by Li *et al.* [14] for the magnetic moment of the Mn atoms on the Ga sublattice. The antiferromagnetic coupling between nearest-neighbor Mn atoms in $Ni_2(Mn_{1-y}Cu_y)(Ga_{1-y}Mn_y)$ alloys is due to the variation of the exchange interaction that becomes antiferromagnetic for small Mn-Mn interatomic distances. This antiferromagnetic coupling was already proved experimentally and theoretically in many Mn-rich Ni-Mn-Ga Heusler alloys [14,23–27]. Then, the μ_s of $Ni_2(Mn_{1-y}Cu_y)(Ga_{1-y}Mn_y)$ alloys is given by $\mu_s(cal) = 2\mu_{Ni} + (1-y)\mu_{MnI} + y\mu_{Cu} + (1-y)\mu_{Ga} + y\mu_{MnII}$, where μ_{MnI} and μ_{MnII} mean the values of the magnetic moment of the Mn atoms on the Mn sublattice and the Ga sublattice, respectively. The broken line in Figure 5 is the one calculated by using the above equation. As seen in Figure 5, the experimental values are in agreement with those calculated for low *y* concentrations. For samples with high *y* concentrations, however, the experimental values of μ_s deviate from the broken

line in Figure 5. This may be attributed to any concentration dependence of the μ_{MnI}, μ_{MnII} and μ_{Ni} values or occurrence of disorder of the constituent elements associated with the increase of y.

In the above considerations on $Ni_2MnGa_{1-y}Cu_y$ $(0 \leq y \leq 0.25)$ alloys, we excluded the site-occupation configurations of $(Ni_{2-y}Cu_y)(Mn_{1-y}Ni_y)(Ga_{1-y}Mn_y)$ and $(Ni_{2-y}Mn_y)(Mn_{1-y}Cu_y)(Ga_{1-y}Ni_y)$ by taking into account the theoretical result that the formation energies of the site-occupations in $Ni_2Mn(Ga_{0.95}Cu_{0.05})$ and $Ni_2(Mn_{0.95}Cu_{0.05})(Ga_{0.95}Mn_{0.05})$ are much smaller than those of $(Ni_{1.95}Cu_{0.05})(Mn_{0.95}Ni_{0.05})(Ga_{0.95}Mn_{0.05})$ and $(Ni_{1.95}Mn_{0.05})(Mn_{0.95}Cu_{0.05})(Ga_{0.95}Ni_{0.05})$ [14]. Unfortunately, the calculations in [14] were made for the site occupation of Cu-doped Ni_2MnGa with the $L2_1$-type structure, instead of the one with the observed martensitic structure at 5 K. Nevertheless, the above satisfactory agreements between the experimental and calculated concentration dependence of the magnetic moment μ_s may rather confirm that the site-occupation configurations in the present analyses exist also in the martensite phase. Lastly, we consider the concentration dependence of μ_s for $Ni_{2-z}Cu_zMnGa$ $(0 \leq z \leq 0.40)$ alloys. As shown in Figure 5, the experimental values of μ_s for $Ni_{2-z}Cu_zMnGa$ $(0 \leq z \leq 0.40)$ alloys are almost independent of concentration z [12]. We assume that Cu atoms for $Ni_{2-z}Cu_zMnGa$ $(0 \leq z \leq 0.40)$ alloys occupy the vacant Ni sublattice according to the results of the calculation by Li *et al.* [14]. Furthermore, we assume that μ_{Ni}, μ_{Cu}, μ_{Mn} and μ_{Ga} in $Ni_{2-z}Cu_zMnGa$ $(0 \leq z \leq 0.40)$ alloys, respectively, are the constant values 0.32 μ_B, 0.04 μ_B, 3.37 μ_B and -0.05 μ_B, which are the magnetic moments calculated by Li *et al.* [14] for $Ni_{1.95}Cu_{0.05}MnGa$. Then, the concentration dependence of $\mu_s(cal)$ for FSMAs $Ni_{2-z}Cu_zMnGa$ $(0 \leq z \leq 0.40)$ alloys is given by $\mu_s(cal) = (2-z)\mu_{Ni} + z\mu_{Cu} + \mu_{Mn} + \mu_{Ga}$, which is shown by the dot dash line in Figure 5. As seen in Figure 5, the experimental values are in good agreement with those calculated.

4. Summary

The magnetization measurements at 5 K of FSMAs $Ni_2Mn_{1-x}Cu_xGa$ $(0 \leq x \leq 0.40)$ and $Ni_2MnGa_{1-y}Cu_y$ $(0 \leq y \leq 0.25)$ alloys have been carried out. The μ_s at 5 K for $Ni_2Mn_{1-x}Cu_xGa$ $(0 \leq x \leq 0.40)$ alloys decreases linearly with increasing concentration x. On the other hand, the μ_s at 5 K for $Ni_2MnGa_{1-y}Cu_y$ $(0 \leq y \leq 0.25)$ alloys decreases steeply with increasing y compared to the μ_s for $Ni_2Mn_{1-x}Cu_xGa$ $(0 \leq x \leq 0.40)$ alloys. To explain the concentration dependence of μ_s for the Cu-modified Ni_2MnGa alloys, we suggested the site-occupation configurations, $Ni_2(Mn_{1-x}Cu_x)Ga$ for $Ni_2Mn_{1-x}Cu_xGa$ $(0 \leq x \leq 0.40)$, $Ni_2(Mn_{1-y}Cu_y)(Ga_{1-y}Mn_y)$ for $Ni_2MnGa_{1-y}Cu_y$ $(0 \leq y \leq 0.25)$ and $(Ni_{2-z}Cu_z)MnGa$ for $Ni_{2-z}Cu_zMnGa$ $(0 \leq z \leq 0.40)$ alloys. These configurations together with some theoretical values of the magnetic moments of constituent atoms were proved to explain well the concentration dependence of μ_s for Cu-modified Ni_2MnGa.

References

1. *Magnetism and Structure in Functional Materials*; Planes, A., Mañosa, L., Saxena, A., Eds.; Springer-Verlag: Berlin Heidelberg, Germany, 2005.
2. *Advances in Magnetic Shape Memory Materials*; Chernenko, V.A., Ed.; Trans. Tech. Publications LTD: Zurich, Switzerland, 2011.
3. Ullakko, K.; Huang, J.K.; Kantner, C.; O'Handley, R.C.; Kokorin, V.V. Large magnetic-field-induced strains in Ni_2MnGa single crystals. *Appl. Phys. Lett.* **1996**, *69*, 1966–1969.
4. Sozinov, A.; Likhachev, A.A.; Lanska, N.; Ullakko, K. Giant magnetic-field-induced strain in NiMnGa seven-layered martensitic phase. *Appl. Phys. Lett.* **2002**, *80*, 1746–1749.
5. Pareti, L.; Solzi, M.; Albertini, F.; Paoluzi, A. Giant entropy change at the co-occurrence of structural and magnetic transitions in the $Ni_{2.19}Mn_{0.81}Ga$ Heusler alloy. *Eur. Phys. J. B* **2003**, *32*, 303–307.
6. Planes, A.; Mañosa, L.; Acet, M. Magnetocaloric effect and its relation to shape-memory properties in ferromagnetic Heusler alloys. *J. Phys. Condens. Matter.* **2009**, *21*, 233201.
7. Webster, P.J.; Ziebeck, K.R.A.; Town, S.L.; Peak, M.S. Magnetic order and phase transformation in Ni_2MnGa. *Phil. Mag. B* **1984**, *49*, 295–310.
8. Brown, P.J.; Crangle, J.; Kanomata, T.; Matsumoto, M.; Neumann, K.-U.; Ouladdiaf, B.; Ziebeck, K.R.A. The crystal structure and phase transitions of the magnetic shape memory compound Ni_2MnGa. *J. Phys. Condens. Matter* **2002**, *14*, 10159.
9. Kataoka, M.; Endo, K.; Kudo, N.; Kanomata, T.; Nishihara, H.; Shishido, T.; Umetsu, R.Y.; Nagasako, M.; Kainuma, R. Martensitic transition, ferromagnetic transition, and their interplay in the shape memory alloys $Ni_2Mn_{1-x}Cu_xGa$. *Phys. Rev. B* **2010**, *82*, 214423.
10. Endo, K.; Kanomata, T.; Kimura, A.; Kataoka, M.; Nishihara, H.; Umetsu, R.Y.; Obara, K.; Shishido, T.; Nagasako, M.; Kainuma, R.; *et al*. Magnetic phase diagram of the ferromagnetic shape memory alloys $Ni_2MnGa_{1-x}Cu_x$. *Mater. Sci. Forum* **2011**, *684*, 165–176.
11. Khovaylo, V.V.; Buchelnikov, V.D.; Kainuma, R.; Koledov, V.V.; Ohtsuka, M.; Shavrov, V.G.; Takagi, T.; Taskaev, S.V.; Vasiliev, A.N. Phase transitions in $Ni_{2+x}Mn_{1-x}Ga$ with a high Ni excess *Phys. Rev. B* **2005**, *72*, 224408.
12. Kanomata, T.; Nozawa, T.; Kikuchi, D.; Nishihara, H.; Koyama, K.; Watanabe, K. Magnetic properties of ferromagnetic shape memory alloys $Ni_{2-x}Cu_xMnGa$. *Int. J. Appl. Electro. Mech.* **2005**, *21*, 151–157.
13. Ahuja, B.L.; Sharma, B.K.; Mathur, S.; Heda, N.L.; Itou, M.; Andrejczuk, A.; Sakurai, Y.; Chakrabarti, A.; Banik, S.; Awasthi, A.M.; *et al*. Magnetic Compton scattering study of $Ni_{2+x}Mn_{1-x}Ga$ ferromagnetic shape-memory alloys. *Phys. Rev. B* **2007**, *75*, 134403.
14. Li, C.M.; Luo, H.B.; Hu, Q.M.; Yang, R.; Johansson, B.; Vitos, L. Site preference and elastic properties of Fe-, Co-, and Cu-doped Ni_2MnGa shape memory alloys from first principles. *Phys. Rev. B* **2011**, *84*, 024206.
15. Fujii, S.; Ishida, S.; Asano, S. Electronic structure and lattice transformation in Ni_2MnGa and Co_2NbSn. *J. Phys. Soc. Jpn.* **1989**, *58*, doi:10.1143/JPSJ.58.3657.
16. Ayuela, A.; Enkovaara, J.; Ullakko, K.; Nieminen, R.M. Structural properties of magnetic Heusler alloys. *J. Phys. Condens. Matter* **1999**, *11*, doi:10.1088/0953-8984/11/8/014.

17. Velikokhatnyĭ, O.I.; Naumov, I.I. Electronic structure and instability of Ni_2MnGa. *Phys. Solid State* **1999**, *41*, 617–623.

18. Godlevsky, V.V.; Rabe, K.M. Soft tetragonal distortions in ferromagnetic Ni_2MnGa and related materials from first principles. *Phys. Rev. B* **2001**, *63*, 134407.

19. Ayuela, A.; Enkovaara, J.; Nieminen, R.M. *Ab initio* study of tetragonal variants in Ni_2MnGa alloy. *J. Phys. Condens. Matter* **2002**, *14*, doi:10.1088/0953-8984/14/21/307.

20. Barman, S.R.; Banik, S.; Chakrabarti, A. Structural and electronic properties of Ni_2MnGa. *Phys. Rev. B* **2005**, *72*, 184410.

21. Kulkova, S.E.; Eremeev, S.V.; Kakeshita, T.; Kulkov, S.S.; Rudenski, G.E. The electronic structure and magnetic properties of full- and half-Heusler alloys. *Mater. Trans.* **2006**, *47*, 599–606.

22. Galanakis, I.; Şaşıoğlu, E. Variation of the magnetic properties of Ni_2MnGa Heusler alloy upon tetragonalization: A first-principles study. *J. Phys. D* **2011**, *44*, 235001.

23. Enkovaara, J.; Heczko, O.; Ayuela, A.; Nieminen, R.M. Coexistence of ferromagnetic and antiferromagnetic order in Mn-doped Ni_2MnGa. *Phys. Rev. B* **2003**, *67*, 212405.

24. Şaşıoğlu, E.; Sandratskii, L.M.; Bruno, P. Pressure dependence of the Curie temperature in Ni_2MnSn Heusler alloy: A first-principles study. *Phys. Rev. B* **2005**, *71*, 214412.

25. Chieda, Y.; Kanomata, T.; Fukushima, K.; Matsubayashi, K.; Uwatoko, Y.; Kainuma, R.; Oikawa K.; Ishida, K.; Obara, K.; Shishido, T. Magnetic properties of Mn-rich Ni_2MnSn Heusler alloys under pressure. *J. Alloys Compd.* **2009**, *486*, 51–54.

26. Khovaylo, V.V.; Kanomata, T.; Tanaka, T.; Nakashima, M.; Amako, Y.; Kainuma, R.; Umetsu, R.Y.; Morito, H.; Miki, H. Magnetic properties of $Ni_{50}Mn_{34.8}In_{15.2}$ probed by Mössbauer spectroscopy. *Phys. Rev. B* **2009**, *80*, 144409.

27. Lázpita, P.; Barandiarán, J.M.; Gutiérrez, J.; Feuchtwanger, J.; Chernenko, V.A.; Richard, M.L. Magnetic moment and chemical order in off-stoichiometric Ni–Mn–Ga ferromagnetic shape memory alloys. *New J. Phys.* **2011**, *13*, 033039.